

---

# Half-VAE: An Encoder-Free VAE to Bypass Explicit Inverse Mapping


---

Yuan-Hao Wei 

Hong Kong Polytechnic University  
Yuan-Hao.Wei@outlook.com

Yan-Jie Sun 

Hong Kong Polytechnic University  
yanjie.sun@connect.polyu.hk

Chen Jason Zhang 

Hong Kong Polytechnic University  
jason-c.zhang@polyu.edu.hk

## Abstract

Inference and inverse problems are closely related concepts, both fundamentally involving the deduction of unknown causes or parameters from observed data. Bayesian inference, a powerful class of methods, is often employed to solve a variety of problems, including those related to causal inference. Variational inference, a subset of Bayesian inference, is primarily used to efficiently approximate complex posterior distributions. Variational Autoencoders (VAEs), which combine variational inference with deep learning, have become widely applied across various domains. This study explores the potential of VAEs for solving inverse problems, such as Independent Component Analysis (ICA), without relying on an explicit inverse mapping process. Unlike other VAE-based ICA methods, this approach discards the encoder in the VAE architecture, directly setting the latent variables as trainable parameters. In other words, the latent variables are no longer outputs of the encoder but are instead optimized directly through the objective function to converge to appropriate values. We find that, with a suitable prior setup, the latent variables, represented by trainable parameters, can exhibit mutually independent properties as the parameters converge, all without the need for an encoding process. This approach, referred to as the Half-VAE, bypasses the inverse mapping process by eliminating the encoder. This study demonstrates the feasibility of using the Half-VAE to solve ICA without the need for an explicit inverse mapping process.

## 1 Introduction

Inverse problems typically involve deducing the system's input or parameters (underlying causes) from observed data (known information). An inverse problem refers to the process of inferring a system's input, parameters, or structure from observed outcomes. The

directly observed information, such as images, sounds, and changes in the surrounding environment, are usually the result of multiple factors acting together (Hyvarinen et al. (2019); Pearl (2019); Khemakhem et al. (2020); Locatello et al. (2020); Schölkopf et al. (2021); Yang et al. (2021); Lachapelle et al. (2022); Schölkopf (2022); Lippe et al. (2022)). When variational inference is applied to inverse problems, it transforms the problem into one of probabilistic inference. Variational Autoencoders (VAEs) combine the principles of variational inference with deep learning (Kingma (2013); Rezende et al. (2014); Kingma and Welling (2019)), endowing them with strong nonlinear mapping capabilities, which in turn provide the potential to tackle complex inference problems. Although causal reasoning, disentanglement, and Independent Component Analysis (ICA) often correspond to different mathematical tools, VAEs have shown remarkable adaptability across these domains (Higgins et al. (2017); Burgess et al. (2018); Chen et al. (2018); Kim and Mnih (2018); Casale et al. (2018); Ramchandran et al. (2021); Brehmer et al. (2022); Tonekaboni et al. (2022); Ahuja et al. (2023); Wei (2024); Wendong et al. (2024)). This demonstrates the powerful generalization capability of variational inference as a mathematical tool when augmented by neural networks. Additionally, obtaining independent latent variables through variational inference can enhance the interpretability of the model, thereby endowing the generative process of VAEs with stronger logic and controllability as a generative model.

Due to the integration of variational Bayesian theory, the encoding process in VAE can be regarded as an inference process. When VAE is designed to solve problems such as ICA or disentanglement, this inference process can be equivalent to an inverse mapping. Briefly, when considering the latent variable  $\mathbf{Z}$  as independent components, the encoding process in a VAE represents the inverse mapping from the mixed observations to the independent components, i.e.,  $\mathbf{Z} = f^{-1}(\mathbf{X})$ . On the other hand, the decoding process in a VAE represents the remapping of the independent components back into the observed data, i.e.,  $\mathbf{X} = f(\mathbf{Z})$ . In many

previous studies, VAE methods for performing disentanglement or ICA typically have a prerequisite that  $M \geq N$  (Casale et al. (2018); Wei (2024)). This is because the encoder struggles to handle situations where the dimensionality  $M$  of the input data  $\mathbf{X}$  is smaller than the dimensionality  $N$  of the latent variable  $\mathbf{Z}$  (also known as the underdetermined case (Comon (1994))). Under underdetermined conditions, the inverse mapping  $\mathbf{f}^{-1}$  is theoretically nonexistent (Cardoso (1998); Bofill and Zibulevsky (2001); Hyvarinen et al. (2001); Cichocki (2002)). Therefore, a strategy is needed to bypass the explicit inverse mapping process in the VAE architecture.

This study discards the encoder in the VAE architecture, allowing the posterior distributions of the latent variables to be directly obtained through trainable parameters converging based on the objective function. This encoder-free VAE is referred to as Half-VAE. We use several randomly generated independent and identically distributed (i.i.d.) signals as the independent components and select Gaussian Mixture Models (GMM) (Dempster et al. (1977); McLachlan (2000); Bishop (2006); Reynolds et al. (2009)) as the prior distributions, with the GMM parameters set as optimizable, adaptive parameters. In this design, the parameters of the posterior and prior distributions of the latent variables, as well as the decoder’s parameters, are all optimized through the objective function. From the perspective of parameter optimization, a typical VAE requires optimizing the parameters of both the encoder and decoder, whereas Half-VAE directly optimizes the posterior distributions of the latent variables. We find that even without an encoder, the different dimensions of the Half-VAE’s latent variables can still converge to mutually independent i.i.d. sequences. Discarding the encoder is equivalent to discarding the inverse mapping stage, theoretically leaving only the ‘forward’ process from the independent components to the observed signals in the Half-VAE. In other words, there is no explicit inverse mapping included in the process of inferring the independent components.

The primary contribution of this study is the introduction of the Half-VAE, an innovative encoder-free VAE architecture. We derive the variational lower bound for the Half-VAE, which serves as its objective function, and validate its effectiveness in solving ICA problems through numerical experiments. Our results demonstrate the feasibility of solving ICA without the need for an explicit inverse mapping process, establishing the practicality of this architecture for such tasks.

## 2 Half-VAE

### 2.1 Derivation

For the derivation of the objective function of Half-VAE, the first step is to maximize the log-marginal likelihood of the observed data  $\mathbf{X}$ :

$$\ln p_{\theta}(\mathbf{X}) = \ln \int p_{\theta}(\mathbf{X}, \mathbf{Z}) d\mathbf{Z}, \quad (1)$$

where  $p_{\theta}(\mathbf{X}, \mathbf{Z})$  is the joint distribution of the observed data  $\mathbf{X}$  and the latent variables  $\mathbf{Z}$ . Introducing an implicit distribution  $I(\mathbf{Z})$  to rewrite the log marginal likelihood:

$$\ln p_{\theta}(\mathbf{X}) = \ln \int \frac{p_{\theta}(\mathbf{X}, \mathbf{Z})}{I(\mathbf{Z})} I(\mathbf{Z}) d\mathbf{Z}, \quad (2)$$

where  $I(\mathbf{Z})$  represent the latent variable distributions characterized by trainable parameters. Since the  $\ln$  function is concave, we can use Jensen’s Inequality (Jensen (1906); Cover (1999); Boyd and Vandenberghe (2004)):

$$\ln p_{\theta}(\mathbf{X}) \geq \int I(\mathbf{Z}) \ln \frac{p_{\theta}(\mathbf{X}, \mathbf{Z})}{I(\mathbf{Z})} d\mathbf{Z}. \quad (3)$$

This inequality represents the evidence lower bound (ELBO) of the log-marginal likelihood. We can further expand the joint distribution  $p_{\theta}(\mathbf{X}, \mathbf{Z})$  as a product of the conditional distribution  $p_{\theta}(\mathbf{X}|\mathbf{Z})$  and the prior distribution  $p(\mathbf{Z})$ :

$$\ln p_{\theta}(\mathbf{X}) \geq \int I(\mathbf{Z}) \ln \frac{p_{\theta}(\mathbf{X}|\mathbf{Z})p(\mathbf{Z})}{I(\mathbf{Z})} d\mathbf{Z}. \quad (4)$$

Breaking down the above equation into two terms:

$$\mathbb{E}_{I(\mathbf{Z})}[\ln p_{\theta}(\mathbf{X}|\mathbf{Z})] = \int I(\mathbf{Z}) \ln p_{\theta}(\mathbf{X}|\mathbf{Z}) d\mathbf{Z}, \quad (5)$$

and

$$-D_{\text{KL}}(I(\mathbf{Z})\|p(\mathbf{Z})) = \int I(\mathbf{Z}) \ln \frac{I(\mathbf{Z})}{p(\mathbf{Z})} d\mathbf{Z}, \quad (6)$$

where the first term represents the reconstruction error, i.e., the expected log-likelihood of generating the data  $\mathbf{X}$  given the latent variables  $\mathbf{Z}$ ; the second term is the Kullback-Leibler (KL) divergence between the implicit posterior distribution  $I(\mathbf{Z})$  and the prior distribution  $p(\mathbf{Z})$ , which measures how much  $I(\mathbf{Z})$  deviates from  $p(\mathbf{Z})$ . Finally, the full expression for the variational lower bound can be obtained:

$$\ln p_{\theta}(\mathbf{X}) \geq \mathbb{E}_{I(\mathbf{Z})}[\ln p_{\theta}(\mathbf{X}|\mathbf{Z})] - D_{\text{KL}}(I(\mathbf{Z})\|p(\mathbf{Z})). \quad (7)$$

The above ELBO equation represents a lower bound that need maximizing by optimizing the parameters  $\theta$

and  $I(\mathbf{Z})$ . The goal is for  $I(\mathbf{Z})$  to approximate the true posterior distribution as closely as possible, while ensuring that the log-likelihood of generating the observed data  $\mathbf{X}$  is maximized.

This derivation demonstrates that, even without an explicit encoding process, we can still obtain a variational lower bound similar to that of a standard VAE (Kingma (2013)) by introducing an implicit distribution  $I(\mathbf{Z})$  determined with trainable parameters. This lower bound is used for optimizing the Half-VAE.

In fact, in the VAE loss function, maximizing the ELBO forces  $D_{\text{KL}}(q(\mathbf{Z}|\mathbf{X})||p(\mathbf{Z}|\mathbf{X}))$  to approach zero, thereby making  $q(\mathbf{Z}|\mathbf{X})$  approximate  $p(\mathbf{Z}|\mathbf{X})$ . Here,  $p(\mathbf{Z}|\mathbf{X})$  represents the true posterior of the latent variables, while  $q(\mathbf{Z}|\mathbf{X})$  is an additional term introduced for approximation. In typical VAEs, this introduced  $q(\mathbf{Z}|\mathbf{X})$  is represented by the encoder, which maps directly from  $\mathbf{X}$  to  $\mathbf{Z}$ . However, in the theoretical derivation of variational inference, the term used to approximate  $p(\mathbf{Z}|\mathbf{X})$  does not necessarily have to be  $q(\mathbf{Z}|\mathbf{X})$ . In this study,  $I(\mathbf{Z})$  is directly used to approximate  $p(\mathbf{Z}|\mathbf{X})$ . Although the explicit encoding process is removed, the core principle of variational inference remains unchanged.

## 2.2 Architecture

Assume that  $\mathbf{X} \in \mathbb{R}^{M \times L}$  is a observable sample with  $M$  features, where  $L$  denotes the length of the features across the different dimensions. We aim to decompose this observable sample into mutually independent components  $\mathbf{Z} \in \mathbb{R}^{N \times L}$ , where  $N$  represents the number of independent components. Within the framework of variational Bayesian inference, the independent components  $\mathbf{Z} \in \mathbb{R}^{N \times L}$  are expressed probabilistically, with means  $\mathbf{Z}_\mu \in \mathbb{R}^{N \times L}$  and variances  $\mathbf{Z}_\sigma \in \mathbb{R}^{N \times 1}$ . Figures 1 and 2 illustrate the schematic diagrams of the process for solving the ICA problem using the traditional VAE architecture and the Half-VAE architecture, respectively. In a VAE, the mean and variance of the latent variables are produced by the encoder, with the encoding process functioning as an explicit inverse mapping. In contrast, in the Half-VAE, the latent variables are treated as trainable parameters that are directly optimized based on the objective function. While the goal of the Half-VAE is also to infer the distribution of the latent variables, it achieves this without an explicit inverse mapping process.

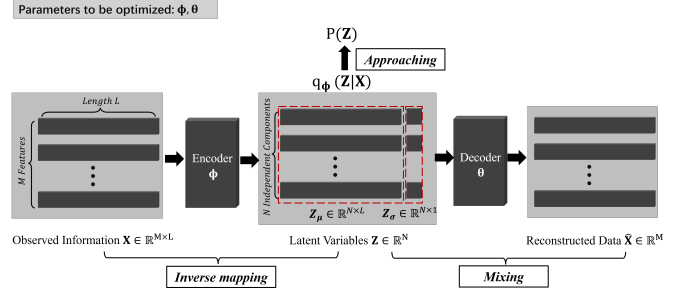


Figure 1: Schematic of VAE

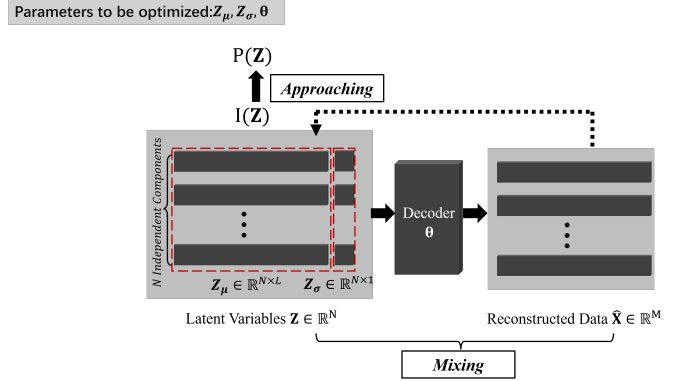


Figure 2: Schematic of Half-VAE

## 2.3 GMM prior

From the objective function (Equation 7), it becomes clear that a well-suited prior distribution is crucial for effective inference of the latent variables  $\mathbf{Z}$ . Therefore, instead of using the standard normal distribution commonly employed in typical VAE framework (Kingma (2013)), we opt for GMMs as the priors for the latent variables. The standard normal distribution lacks the flexibility needed to capture the complex, unknown distributions of the independent components. In contrast, GMMs, as powerful probabilistic models, excel at fitting complex distributions and are not restricted by the limitations of a single Gaussian component, making them more adaptable to intricate data structures and flexible distributional assumptions.

A Gaussian Mixture Model (GMM) is defined as:

$$p(\mathbf{Z}) = \sum_{k=1}^K \pi_k \mathcal{N}(\mathbf{Z} | m_k, \Sigma_k) \quad (8)$$

where  $\pi_k$  are the mixture weights,  $\mu_k$  are the means, and  $\Sigma_k$  are the covariances for each component  $k$  of the GMM. Given that the true distributions of the independent components in the ICA problem are unknown, we cannot directly assign precise parameters to the GMM priors. However, we can design these parameters  $\boldsymbol{\pi}$ ,  $\boldsymbol{m}$ ,

and  $\Sigma$  as trainable variables, allowing their values to be optimized through the objective function. For simplicity, we set the weights  $\pi$ , means  $m$ , and covariances  $\Sigma$  are elements of the parameter set  $\Psi$ , i.e.,  $\pi, m, \Sigma \in \Psi$ . Consequently, the loss functions for the VAE and Half-VAE with GMM priors can be further expressed as follows:

$$L_{\text{VAE}}(\phi, \theta, \Psi; \mathbf{X}) = -\mathbb{E}_{q_{\phi}(\mathbf{Z}|\mathbf{X})} [\ln p_{\theta}(\mathbf{X}|\mathbf{Z})] + \lambda \cdot D_{\text{KL}} [q_{\phi}(\mathbf{Z}|\mathbf{X}) \| \text{GMM}_{\Psi}(\mathbf{Z})], \tag{9}$$

$$L_{\text{Half-VAE}}(\mathbf{Z}_{\mu}, \mathbf{Z}_{\sigma}, \theta, \Psi; \mathbf{X}) = -\mathbb{E}_{I(\mathbf{Z})} [\ln p_{\theta}(\mathbf{X}|\mathbf{Z})] + \lambda \cdot D_{\text{KL}} (I(\mathbf{Z}) \| \text{GMM}_{\Psi}(\mathbf{Z})), \tag{10}$$

where  $\lambda$  is used to adjust the weights of each item in the loss functions. The  $I(\mathbf{Z})$  directly represented by  $\mathbf{Z}_{\mu}$  and  $\mathbf{Z}_{\sigma}$ . Note that, for the convenience of performing stochastic gradient descent in neural networks, we have reformulated the maximization of the ELBO (see Equation 7) into the minimization of the negative ELBO as loss functions, as shown in Equations 8 and 9.

### 3 Experiments

To evaluate the ability of the proposed Half-VAE to solve the ICA problem, we design a set of simulation experiments. First, multiple random signals are generated, as shown in Figure 3. During the generation process, efforts are made to make these signals as independent from each other as possible. After passing through a mixing mapping, we obtain the mixed observations, as illustrated in Figure 4. Without knowledge of the ground truth, the independent components are inferred in an unsupervised manner using both the VAE and Half-VAE.

The number of Gaussian distributions in the GMM prior for each independent component is empirically set to 3, i.e.,  $k = 3$ . The parameters of both the VAE and Half-VAE are optimized according to their loss functions, respectively. Figure 5 illustrates the evolution of  $\mathbf{Z}_{\mu}$  over epochs. It can be observed that  $\mathbf{Z}_{\mu}$  gradually approaches the true independent components as the Half-VAE model is optimized effectively.

It is important to note that in both Half-VAE and VAE, the latent variables are represented probabilistically, meaning that the inferred independent components are distributions rather than fixed values. Figure 6 shows the distribution of each independent component inferred by the Half-VAE after the loss function has converged, denoted as  $I(\mathbf{Z})$ . The pink lines represent the mean of each independent component, while the gray shaded areas indicate the 95% confidence intervals. It

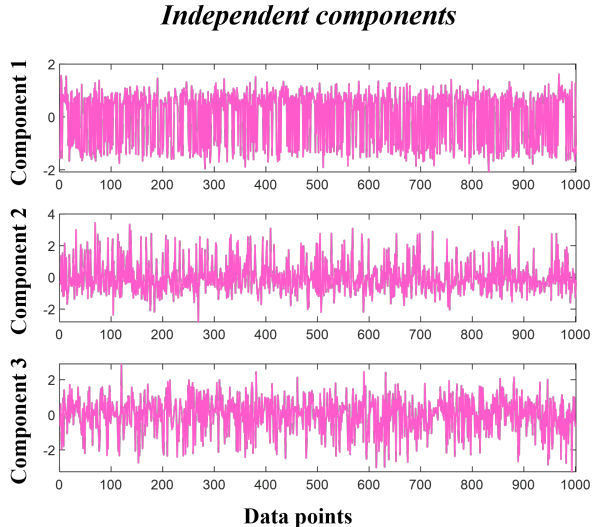


Figure 3: Independent components

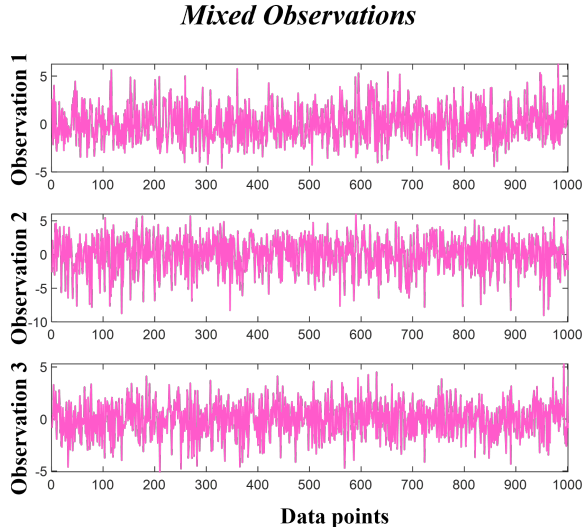


Figure 4: Observations

can be observed that the model exhibits relatively low uncertainty in the estimated results, as the confidence intervals are quite narrow.

The inference results of the Half-VAE and VAE are shown in Figures 7 and 8. For a broader comparison, we also evaluate the performance of a vanilla VAE, following the original settings for ICA. The prior of the vanilla VAE is set to a standard normal distribution (Kingma (2013)) rather than a GMM. The results for the vanilla VAE are shown in Figure 9. Due to the inherent scaling ambiguity in ICA solutions (Comon (1994); Hyvarinen et al. (2001)), we apply the z-score normalization method (Altman (1992); Iglewicz and Hoaglin (1993)) to both the true independent components and



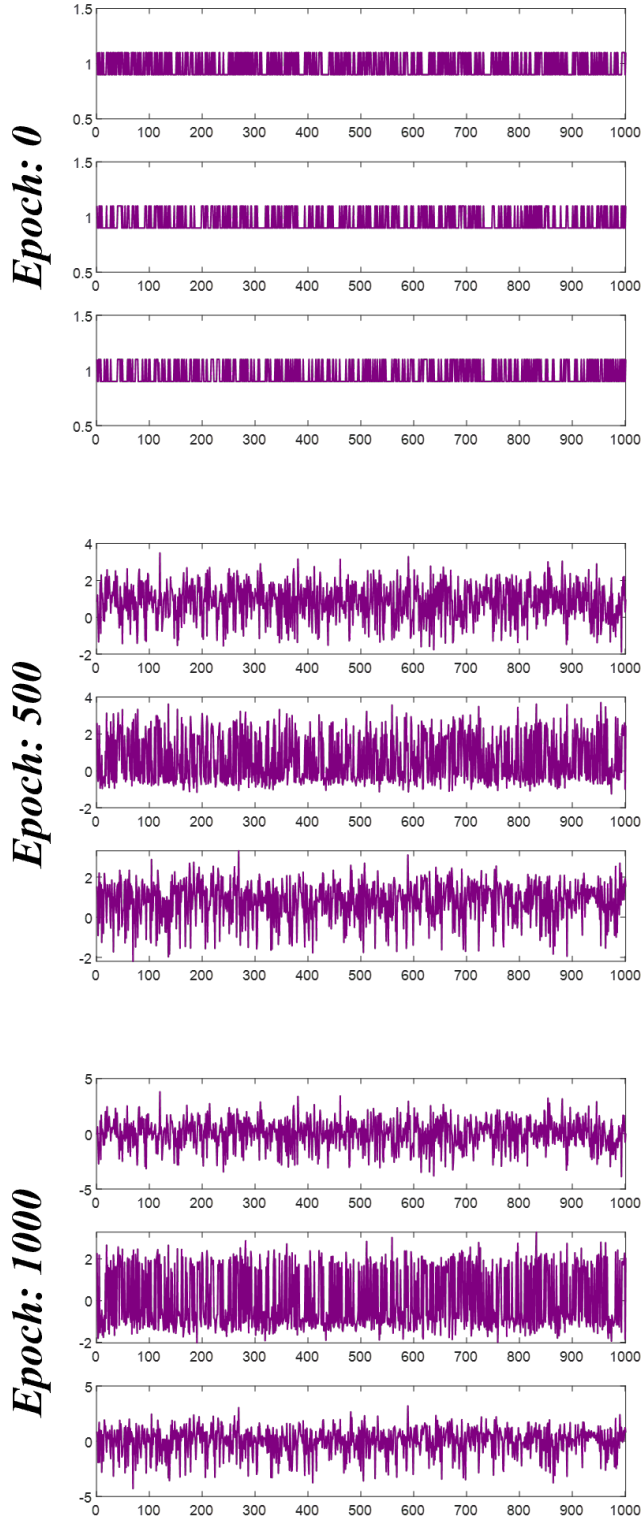
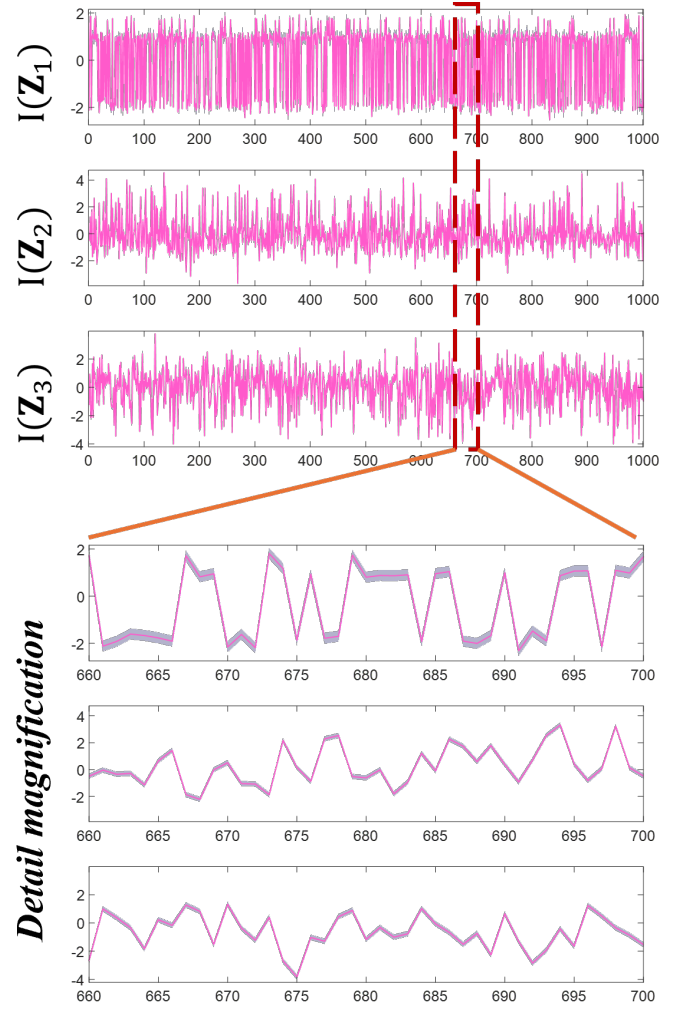

 Figure 5: The change of  $\mathbf{Z}_\mu$  with epoch


Figure 6: Estimated distributions of independent components

the estimated results to compare them on the same scale. In these figures, the purple solid lines represent the normalized ground truth independent components, while the green dashed lines represent the means of the inferred independent component distributions for each model. It can be observed that both the Half-VAE and the VAE with GMM priors accurately infer the independent components, whereas the results from the vanilla VAE deviate significantly from the ground truth. The root mean square errors (RMSE) between the inferred results and the corresponding ground truth for each model are presented in Table 1.

## 4 Discussions and future works

This study proposes a novel VAE architecture, the Half-VAE, and derives its variational lower bound, which

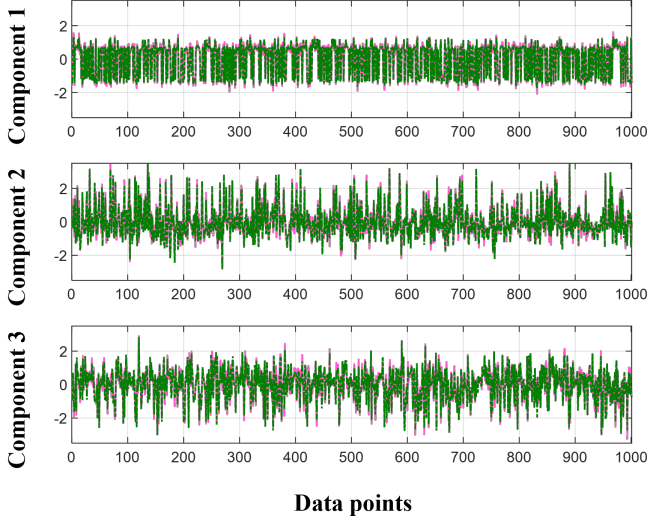


Figure 7: ICA performance of Half-VAE

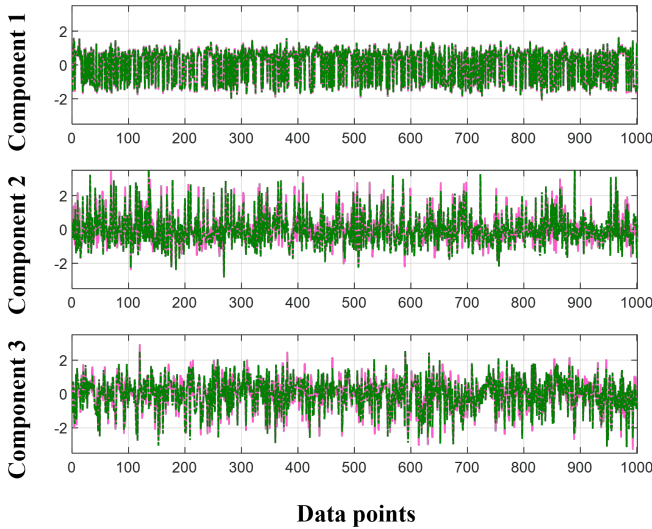


Figure 8: ICA performance of VAE(GMM)

Table 1: Comparison of the accuracy of inference between Half-VAE, VAE, and Vanilla VAE in solving ICA problems

	Half-VAE(GMM)	VAE(GMM)	Vanilla VAE
Component 1	0.1174	0.0371	0.7195
Component 2	0.2023	0.3942	0.6102
Component 3	0.2342	0.3272	0.7380
Mean	0.1846	0.2528	0.6892

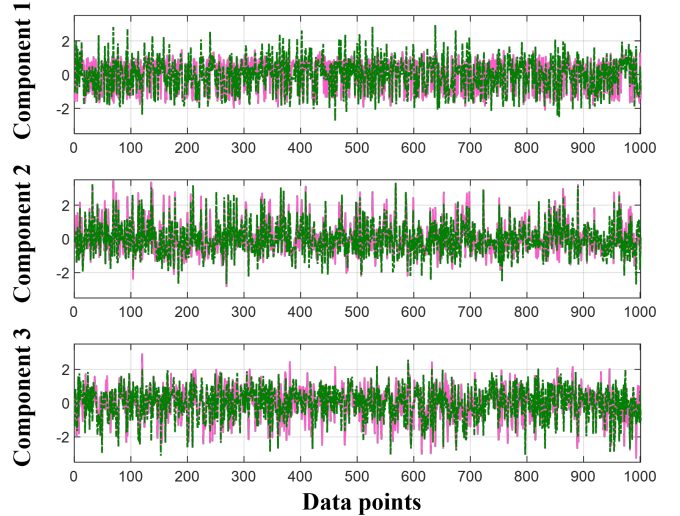


Figure 9: ICA performance of Vanilla VAE

also serves as the objective function. Unlike the traditional VAE architecture, the Half-VAE discards the encoder, with the latent variables directly represented by trainable parameters that are optimized through the loss function. Since the Half-VAE does not have the encoding process present in a VAE, it avoids the need for explicit inverse mapping. Our experiments demonstrate that the Half-VAE performs comparably to the traditional VAE in solving ICA problems.

However, several issues require further investigation. At the current stage of research, the Half-VAE still cannot directly achieve ICA under underdetermined conditions. Although the Half-VAE avoids explicit inverse mapping, solving underdetermined problems still requires more assumptions and constraints depending on the various conditions (Comon (1994); Hyvarinen et al. (2001)). Additionally, we found that the random initialization of parameters in both the Half-VAE and VAE architectures plays a crucial role in how quickly the models converge. Thus, future work will also investigate the design of effective initialization strategies for both Half-VAE and VAE in solving ICA problems.

## Acknowledgments

This research was supported by the project Data integration with dialogue systems (1-52JM). We would like to thank the project for its funding and support, which has made this work possible.

## References

- Ahuja, K., Mahajan, D., Wang, Y., and Bengio, Y. (2023). Interventional causal representation learning. In *International conference on machine learning*, pages 372–407. PMLR.
- Altman, N. S. (1992). An introduction to kernel and nearest-neighbor nonparametric regression. *The American Statistician*, 46(3):175–185.
- Bishop, C. M. (2006). Pattern recognition and machine learning. *Springer google schola*, 2:1122–1128.
- Bofill, P. and Zibulevsky, M. (2001). Underdetermined blind source separation using sparse representations. *Signal processing*, 81(11):2353–2362.
- Boyd, S. and Vandenberghe, L. (2004). *Convex optimization*. Cambridge university press.
- Brehmer, J., De Haan, P., Lippe, P., and Cohen, T. S. (2022). Weakly supervised causal representation learning. *Advances in Neural Information Processing Systems*, 35:38319–38331.
- Burgess, C. P., Higgins, I., Pal, A., Matthey, L., Watters, N., Desjardins, G., and Lerchner, A. (2018). Understanding disentangling in  $\beta$ -vae. *arXiv preprint arXiv:1804.03599*.
- Cardoso, J.-F. (1998). Blind signal separation: statistical principles. *Proceedings of the IEEE*, 86(10):2009–2025.
- Casale, F. P., Dalca, A., Saglietti, L., Listgarten, J., and Fusi, N. (2018). Gaussian process prior variational autoencoders. *Advances in neural information processing systems*, 31.
- Chen, R. T., Li, X., Grosse, R. B., and Duvenaud, D. K. (2018). Isolating sources of disentanglement in variational autoencoders. *Advances in neural information processing systems*, 31.
- Cichocki, A. (2002). Adaptive blind signal and image processing: Learning algorithms and applications. *John Wiley & Sons google schola*, 2:1129–1159.
- Comon, P. (1994). Independent component analysis, a new concept? *Signal processing*, 36(3):287–314.
- Cover, T. M. (1999). *Elements of information theory*. John Wiley & Sons.
- Dempster, A. P., Laird, N. M., and Rubin, D. B. (1977). Maximum likelihood from incomplete data via the em algorithm. *Journal of the royal statistical society: series B (methodological)*, 39(1):1–22.
- Higgins, I., Matthey, L., Pal, A., Burgess, C. P., Glorot, X., Botvinick, M. M., Mohamed, S., and Lerchner, A. (2017). beta-vae: Learning basic visual concepts with a constrained variational framework. *ICLR (Poster)*, 3.
- Hyvarinen, A., Karhunen, J., and Oja, E. (2001). Independent component analysis and blind source separation.
- Hyvarinen, A., Sasaki, H., and Turner, R. (2019). Non-linear ica using auxiliary variables and generalized contrastive learning. In *The 22nd International Conference on Artificial Intelligence and Statistics*, pages 859–868. PMLR.
- Iglewicz, B. and Hoaglin, D. C. (1993). *Volume 16: how to detect and handle outliers*. Quality Press.
- Jensen, J. L. W. V. (1906). Sur les fonctions convexes et les inégalités entre les valeurs moyennes. *Acta mathematica*, 30(1):175–193.
- Khemakhem, I., Kingma, D., Monti, R., and Hyvarinen, A. (2020). Variational autoencoders and nonlinear ica: A unifying framework. In *International conference on artificial intelligence and statistics*, pages 2207–2217. PMLR.
- Kim, H. and Mnih, A. (2018). Disentangling by factorising. In *International conference on machine learning*, pages 2649–2658. PMLR.
- Kingma, D. P. (2013). Auto-encoding variational bayes. *arXiv preprint arXiv:1312.6114*.
- Kingma, D. P. and Welling, M. (2019). An introduction to variational autoencoders. arxiv e-prints, page. *arXiv preprint arXiv:1906.02691*.
- Lachapelle, S., Rodriguez, P., Sharma, Y., Everett, K. E., Le Priol, R., Lacoste, A., and Lacoste-Julien, S. (2022). Disentanglement via mechanism sparsity regularization: A new principle for nonlinear ica. In *Conference on Causal Learning and Reasoning*, pages 428–484. PMLR.
- Lippe, P., Magliacane, S., Löwe, S., Asano, Y. M., Cohen, T., and Gavves, S. (2022). Citris: Causal identifiability from temporal intervened sequences. In *International Conference on Machine Learning*, pages 13557–13603. PMLR.
- Locatello, F., Poole, B., Rätsch, G., Schölkopf, B., Bachem, O., and Tschannen, M. (2020). Weakly-supervised disentanglement without compromises. In *International conference on machine learning*, pages 6348–6359. PMLR.
- McLachlan, G. J. (2000). Finite mixture models. *A wiley-interscience publication*.

- Pearl, J. (2019). The seven tools of causal inference, with reflections on machine learning. *Communications of the ACM*, 62(3):54–60.
- Ramchandran, S., Tikhonov, G., Kujanpää, K., Koskinen, M., and Lähdesmäki, H. (2021). Longitudinal variational autoencoder. In *International Conference on Artificial Intelligence and Statistics*, pages 3898–3906. PMLR.
- Reynolds, D. A. et al. (2009). Gaussian mixture models. *Encyclopedia of biometrics*, 741(659-663).
- Rezende, D. J., Mohamed, S., and Wierstra, D. (2014). Stochastic backpropagation and approximate inference in deep generative models. In *International conference on machine learning*, pages 1278–1286. PMLR.
- Schölkopf, B. (2022). Causality for machine learning. In *Probabilistic and causal inference: The works of Judea Pearl*, pages 765–804.
- Schölkopf, B., Locatello, F., Bauer, S., Ke, N. R., Kalchbrenner, N., Goyal, A., and Bengio, Y. (2021). Toward causal representation learning. *Proceedings of the IEEE*, 109(5):612–634.
- Tonekaboni, S., Li, C.-L., Arik, S. O., Goldenberg, A., and Pfister, T. (2022). Decoupling local and global representations of time series. In *International Conference on Artificial Intelligence and Statistics*, pages 8700–8714. PMLR.
- Wei, Y. (2024). *Innovative Blind Source Separation Techniques Combining Gaussian Process Algorithms and Variational Autoencoders with Applications in Structural Health Monitoring*. Ph.d. dissertation, Hong Kong Polytechnic University, Hong Kong.
- Wendong, L., Kekić, A., von Kügelgen, J., Buchholz, S., Besserve, M., Gresele, L., and Schölkopf, B. (2024). Causal component analysis. *Advances in Neural Information Processing Systems*, 36.
- Yang, M., Liu, F., Chen, Z., Shen, X., Hao, J., and Wang, J. (2021). Causalvae: Disentangled representation learning via neural structural causal models. In *Proceedings of the IEEE/CVF conference on computer vision and pattern recognition*, pages 9593–9602.